IEICE TRANS. COMMUN., VOL.E83–B, NO.8 AUGUST 2000

PAPER *Special Issue on Personal, Indoor and Mobile Radio Communications*

Proposal of Radio-over-Fiber Systems Using Cascaded Radio-to-Optic Direct Conversion Scheme

Pat SUWONPANICH[†], ***Student Member***, **Katsutoshi TSUKAMOTO**[†], ***and*** **Shozo KOMAKI**[†], ***Regular Members***

SUMMARY This paper newly proposes radio-over-fiber systems using cascaded radio-to-optic direct conversion (ROC) scheme. The ROC system can convert a radio signal into an optical signal with the same signal format. The received carrier-to-noise ratio (CNR) performance of the radio-over-fiber systems using the ROC/heterodyne detection (HD) scheme and the ROC/self-heterodyne detection (SHD) scheme are theoretically analyzed. The optimization of an optical modulation index (OMI) in each radio base station (RBS) is also presented. By using the proposed OMI optimization method, the ROC/HD and the ROC/SHD schemes are shown to provide approximately 16 dB and 14 dB improvement over the intensity modulation/direct detection scheme when the number of RBS is 20 and the radio-frequency (RF) signal bandwidth is 150 MHz, respectively. The ROC/SHD scheme enables a receiver structure to become simple while still achieving high received CNR.

key words: *radio-to-optic direct conversion, radio-over-fiber systems, cascade link, heterodyne detection, self-heterodyne detection*

1. Introduction

Microcellular communication systems have been extensively studied in order to meet the rapidly increasing demand for mobile communications. The systems contain smaller cells (microcells) and promise effective frequency utilization, thus satisfy the escalating demand. However, the number of radio base stations (RBSs) has been increased in order to start new kinds of radio service and to accommodate more subscribers. Moreover, as the microcell size shrinks, a large number of RBSs are required in order to cover a given area. Therefore, it is essential to develop simpler RBSs. Radio-over-fiber systems have been widely researched recently [1], [2]. In radio-over-fiber systems, radio signals in micro-cells are encapsulated into an optical signal envelope and then transferred to their destinations through optical fibers (Fig. 1). All of the modulators/demodulators and system control circuitry are relocated away from the RBS to a control station (CS), therefore the RBS becomes simple. As the baseband modulation/demodulation is not implemented in the RBSs, therefore the RBSs and backyard optic-fiber networks can be used for various types of radio services flexibly, so the number of RBSs can be much reduced.

Regarding optical modulation schemes for radio signals, intensity modulation/direct detection (IM/DD) systems have been mainly considered from the viewpoint of its technical and economical implementation [3]–[7]. Among these systems, radio-over-fiber systems employing star-type inter-cell connection link [4], [5] and radio-over-fiber systems employing bus-type inter-cell connection link [6], [7] have been widely studied. However, beat noises occur in both star-type and bus-type systems because several laser diodes (LD) are used. Consequently, the optical transmission performances are severely deteriorated.

To solve the problem above, it is required that only one light source is used in the system. One solution is to employ a cascade-type inter-cell connection link. The cascaded intensity modulation/direct de-

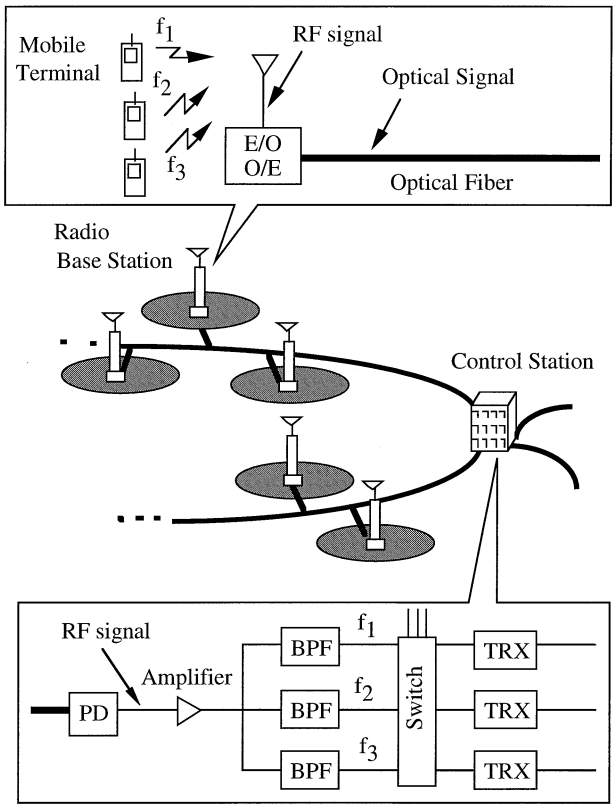

Fig. 1 Radio-over-fiber system.

Manuscript received December 10, 1999.
Manuscript revised March 18, 2000.

[†]The authors are with the Department of Communications Engineering, Osaka University, Suita-shi, 565-0871 Japan.

tection (IM/DD) scheme and cascaded phase modulation/heterodyne detection (PM/HD) scheme have been proposed in [8], [9], respectively. However, the conventional cascade-link transmission performance suffers severely from intermodulation distortion even if only one radio subcarrier is used per RBS, since all of the optical carrier and signals from previous RBSs are modulated together in the RBS.

In this paper, we propose a novel cascaded radio-over-fiber system. In the proposed systems, the optical pilot carrier is divided from all signals modulated by radio signals at previous RBSs by the use of a frequency splitter. After that, the optical modulator converts a radio signal at the current RBS to an optical signal by modulating only the pilot carrier. Then, by the use of a frequency combiner, the optical carrier and all optical signals are combined together again. Therefore no intermodulation distortion due to cascaded modulators occurs in the systems [10]–[12]. Also, no beat noise caused by the use of several light sources occurs. For modulation, we employ the radio-to-optic direct conversion (ROC) scheme [13], [14]. ROC has been studied for coherent optical transmission systems which can approach the shot noise limited performance, make up considerably dense optical frequency division multiplexing signals, and detect frequency or phase of the optical carrier. Furthermore, ROC can convert microwave or millimeter-wave signals into optical signals with their signal formats kept and without any baseband demodulation or modulation.

In the conventional cascaded IM/DD system, the intermodulation distortion due to cascaded modulators occurs even if only one radio subcarrier is used per RBS and the modulation has an ideal linearity. Therefore, to analyze the fundamental merit of the proposed system, one radio subcarrier per RBS is assumed in this study.

When the number of radio subcarriers is more than 1, the intermodulation distortion is induced by the nonlinearity of the ROC modulator. The investigation of this distortion has been performed in Ref. [14]. However, the merit of the proposed cascade system still remains, because the merit is to eliminate the carrier-to-distortion-plus-noise-power ratio (CDNR) degradation due to the intermodulation distortion induced by the cascaded modulators.

The rest of this paper is organized as follows: In Sect. 2, radio-over-fiber systems using cascaded radio-to-optic direct conversion scheme are introduced and described. The received carrier-to-noise-power ratio (CNR) performance of the proposed systems is theoretically analyzed in Sect. 3. In Sect. 4, the numerical results are shown and discussed. Also, the optical modulation index optimization method is presented. Finally, we summarize our results in Sect. 5.

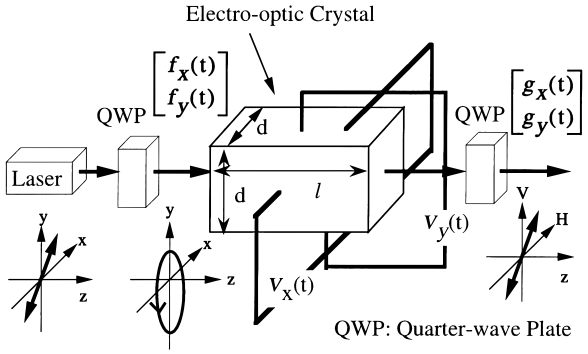

Fig. 2 Configuration of the radio-to-optic direct conversion scheme.

2. Radio-over-Fiber Systems Using Cascaded Radio-to-Optic Direct Conversion Schemes

Figure 2 shows the configuration of the ROC scheme. The right circularly polarized lightwave is inserted along the z axis of the electro-optic crystal such as a $LiNbO_3$ crystal. Also, mutually orthogonal driving voltage, $v_x(t)$ and $v_y(t)$ are applied along x and y axis of the crystal. $v_x(t)$ and $v_y(t)$ are respectively given by

$$v_x(t) = V(t)\sin[2\pi f_{RF}t + \Psi(t)] \tag{1}$$

$$v_y(t) = V(t)\cos[2\pi f_{RF}t + \Psi(t)] \tag{2}$$

where $V(t)$, f_{RF}, and $\Psi(t)$ are the amplitude, frequency and phase of the RF signals, respectively. The output lightwaves, $g_x(t)$ and $g_y(t)$, can be expressed as follows [13]:

$$\begin{aligned}\begin{bmatrix} g_x(t) \\ g_y(t) \end{bmatrix} &= \sqrt{P}\cos\left(\pi\frac{V(t)}{V_\pi}\right)\cdot e^{j[2\pi f_o t-\phi_o+\phi_s(t)]}\begin{bmatrix} -j \\ 1 \end{bmatrix} \\ &\quad -\sqrt{P}\sin\left(\pi\frac{V(t)}{V_\pi}\right) \\ &\quad \cdot e^{j[2\pi(f_o+f_{RF})t+\Psi(t)-\phi_o+\phi_s(t)]}\begin{bmatrix} +j \\ 1 \end{bmatrix}\end{aligned} \tag{3}$$

where P is the average intensity, V_π is the half-wave voltage, f_o is the optical carrier frequency, ϕ_o is the phase constant, and ϕ_s is the phase noise of light source. It is seen from Eq. (3) that the output lightwave is composed of two components. If the amplitude of the RF signal $V(t)$ is small enough to yield $\pi V(t)/V_\pi \ll 1$, the second term on the right hand side of the equation can be seen as a replica of the input RF signal in the optical band, which has the same amplitude and phase as the input RF signal. On the other hand, the first term can be utilized as a pilot carrier because it has non-modulated amplitude and phase.

Figure 3(a) shows the configuration of the cascaded radio-over-fiber system. Figures 3(b) and (c)

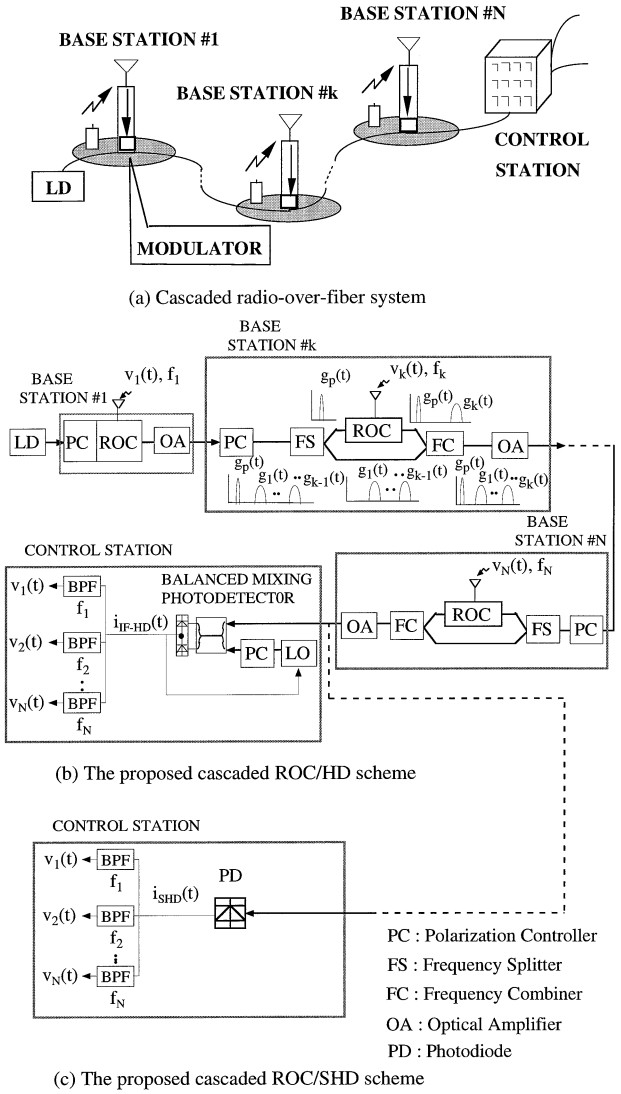

Fig. 3 Configuration of cascaded radio-over-fiber system.

show the proposed cascaded ROC schemes, and also the frequency spectrum of the signal at each stage in the RBS. At the input of an arbitrary k-th RBS, signals from the previous stations: $g_1(t), g_2(t), \ldots, g_{k-1}(t)$, and the pilot carrier, $g_p(t)$, will be transmitted through a polarization controller (PC). Then, in order to prevent the intermodulation distortion, the pilot carrier is divided from the signals $(g_1(t), g_2(t), \ldots, g_{k-1}(t))$ by a frequency splitter (FS). By the use of only the pilot carrier (therefore no intermodulation distortion occurs), the ROC converts the RF signal at the k-th RBS to an optical signal. Then, all optical signals are combined together again by a frequency combiner (FC). After compensating the propagation loss of the optical fiber between RBSs and the insertion loss in an RBS by an optical amplifier, all optical signals are transmitted to the next RBS.

At the CS, in the case of heterodyne detection shown in Fig. 3(b), the received light is detected by a balanced mixing photodetector after matching the polarization of the received light with that of the local oscillator (LO) light by the PC. The RF signals are regenerated after passing through bandpass filters (BPFs). In this case, the frequency control and the state of polarization control of the local oscillator is executed by the use of feedback of the IF signal. On the other hand, in the case of self-heterodyne detection shown in Fig. 3(c), the received light is detected directly by a photodiode and the RF signals are regenerated by the use of BPF. In this case, the pilot carrier and the signals encounter the same polarization fluctuation in the fiber, moreover, phase noises of both of them are also identical. Therefore, phase noises are canceled after detection by the photodiode. Thus, the LO, the frequency control, and the state of polarization control are not necessary and the receiver structure becomes simple.

3. CNR Performance Analysis

In this study, the received CNR of the cascaded ROC systems are theoretically analyzed assuming 1 subcarrier per RBS. The loss between each amplifier can be expressed as follows:

$$L_{sub} = L_f L_s L_m L_d \tag{4}$$

where L_f, L_s, L_m and L_d are the fiber propagation loss between two adjacent RBSs, the insertion loss of the PC, the modulator, and the FS together with the FC, respectively.

To compensate for the losses occuring in the cascaded systems, optical amplifiers are assumed to be inserted after each RBS. The gain of each optical amplifier is set to be identical to all losses between itself and the previous optical amplifier, thus

$$G_1 = \frac{1}{L_s L_m} \quad \text{for the amplifier in the first RBS} \tag{5}$$

$$G = \frac{1}{L_{sub}} \quad \text{for amplifiers in other RBSs} \tag{6}$$

In cascade-link systems, the ASE noises accumulate and are amplified at the following amplifiers. At the receiver input, the accumulated ASE noises can be considered as white noise throughout the total subcarrier signal band, therefore, the ASE noise has the same power density in each RF signal band. Assuming that frequency splitters and frequency combiners can split and combine frequency spectrum perfectly, the power spectral density of the amplified spontaneous emission (ASE) received at the receiver is [15], [16]

$$N_{ASE} = \frac{n_{sp}(G_1 - 1)h\nu + (p-1)n_{sp}(G-1)h\nu}{L_f} \tag{7}$$

where n_{sp}, h, ν, and p are the ASE coefficient, Planck's constant, the optical frequency, and the number of optical amplifiers, respectively.

In the case of heterodyne detection, the LO light is

$$g_L(t) = \sqrt{2P_L}e^{j\{2\pi f_L t+\phi_L(t)\}} \tag{8}$$

where P_L, f_L, and $\phi_L(t)$ are the LO power, the LO frequency, and the LO phase noise, respectively.

The intermediate frequency (IF) current after the balanced mixing photodetector is

$$i_{IF-HD}(t)=i_{C-HD}(t)+\sum_{k=1}^{N} i_{k-HD}(t)+n_{HD}(t) \tag{9}$$

where $i_{C-HD}(t)$, $i_{k-HD}(t)$, N, and $n_{HD}(t)$ are the carrier, the signal from the k-th RBS, the number of RBSs connected in the system, and the noise, respectively. The carrier and the signal from the k-th RBS can be expressed by

$$i_{C-HD} = 2e\alpha\sqrt{P_C P_L}\cdot\cos[2\pi f_{IF}t + \Delta\phi(t)] \tag{10}$$

$$\begin{aligned} i_{k-HD} \;=\; & 2e\alpha\sqrt{P_{r,k}P_L} \\ & \cdot\cos[2\pi(f_{IF}+f_{RF}+k\Delta f)t \\ & +\Delta\phi(t)+\theta_k(t)] \end{aligned} \tag{11}$$

where e, α, P_C, $P_{r,k}$, f_{IF}, f_{RF}, Δf, $\Delta\phi(t)$, and $\theta_k(t)$ are the electron charge, the electro-optic constant, the received power of the pilot carrier, the received optical power of the signal from the k-th RBS, the frequency of the IF signal ($f_{IF} = f_O - f_L$), the subcarrier radio frequency, the frequency interval between two adjacent RF signals , the phase noise of the optical signal ($\Delta\phi(t) = \phi_O(t) - \phi_L(t)$), and the phase of the k-th RF signal, respectively. The received power of the pilot carrier, P_C, and the received optical power of the signal from the k-th RBS, $P_{r,k}$ can be expressed as follows:

$$P_C = P_t L_f \cdot \left[\prod_{k=1}^{N}\cos(\pi OMI_k)\right]^2 \tag{12}$$

$$P_{r,k}=\frac{P_t L_f}{L_m^{(N-k)}}\left[\sin(\pi OMI_k)\cdot\left\{\prod_{j=1}^{k-1}\cos(\pi OMI_j)\right\}\right]^2 \tag{13}$$

where P_t is the transmitting optical power and OMI_k is the optical modulation index (OMI) of the k-th RBS defined by

$$OMI_k = \frac{A_k}{V_\pi} \tag{14}$$

where A_k is the amplitude of the k-th RF signal. Hence, the power of the signal from the k-th RBS is

$$P_{HD,k} = 2e^2\alpha^2 P_{r,k}P_L \tag{15}$$

Considering the relative intensity noise (RIN), ASE noise, the signal and the LO shot noise, and the receiver thermal noise, the total noise power can be given by

$$\begin{aligned} &\sigma^2_{HD,total} \\ &\quad= \Bigg\{ RINe^2\alpha^2 P_r P_L + 2e^2\alpha P_r + 2e^2\alpha P_L \\ &\qquad + 2e^2\alpha N_{ASE}B_o + \frac{8k_BT}{R_L} + 4e^2\alpha^2 P_L N_{ASE} \\ &\qquad + 4e^2\alpha^2 P_r N_{ASE} + 4e^2\alpha^2 N^2_{ASE}B_o \Bigg\} B \end{aligned} \tag{16}$$

where P_r, B_o, k_B, T, R_L and B are the total received optical power, the bandwidth of an optical filter, the Boltzmann constant, the noise temperature, the load resistance, and the RF signal bandwidth, respectively. The eight terms on the right-hand side of Eq. (16) are the RIN, the signal shot noise, the LO shot noise, the ASE shot noise, the receiver thermal noise, the LO-spontaneous emission beat noise, the signal-spontaneous emission beat noise, and the spontaneous-spontaneous emission beat noise, respectively. The total received optical power, P_r, can be written as

$$P_r = P_c + \sum_{k=1}^{N} P_{r,k} \tag{17}$$

Therefore, the received CNR of the RF signal from the k-th RBS is

$$CNR_{HD,k} = \frac{P_{HD,k}}{\sigma^2_{HD,total}} \tag{18}$$

In the case of self-heterodyne detection, the output current after a photodiode is

$$i_{SHD}(t) = \sum_{k=1}^{N} i_{k-SHD}(t) + n_{SHD}(t) \tag{19}$$

where $i_{k-SHD}(t)$ and $n_{SHD}(t)$ are the signal from the k-th RBS and the noise, respectively. The signal from the k-th RBS can be expressed by

$$\begin{aligned} i_{k-SHD} \;=\; & 2e\alpha\sqrt{P_{r,k}P_C} \\ & \cdot\cos[2\pi(f_{RF}+k\Delta f)t+\theta_k(t)] \end{aligned} \tag{20}$$

Hence, the power of the signal from the k-th RBS is given by

$$P_{SHD,k} = 2e^2\alpha^2 P_{r,k}P_C \tag{21}$$

where $P_{r,k}$ is the given by Eq. (13). The total noise power can be written as

$$\sigma^2_{SHD,total} = \left\{ RINe^2\alpha^2P_r^2 + 2e^2\alpha P_r + 2e^2\alpha N_{ASE}B_o + \frac{4k_BT}{R_L} + 4e^2\alpha^2P_rN_{ASE} + 4e^2\alpha^2N^2_{ASE}B_o \right\} B \quad (22)$$

Therefore, the received CNR of the k-th RBS is

$$CNR_{SHD,k} = \frac{P_{SHD,k}}{\sigma^2_{SHD,total}} \quad (23)$$

When the number of subcarrier is more than 1, the CDNR degradation due to the intermodulation distortion induced by the nonlinearity of the modulator occurs. However, the merit of the proposed cascade system still remains, i.e., the system can eliminate the CDNR degradation due to the intermodulation distortion induced by the cascaded modulators.

4. Numerical Results and Discussion

Table 1 shows the parameters used in calculations. In the calculation, the distance between two adjacent RBS is assumed to be 100 m, therefore the fiber propagation loss, L_f, between two adjacent RBS is assumed to be 0.02 dB.

4.1 Using Identical Optical Modulation Index in Every RBS

Figure 4 shows the relationship between the received CNR for ROC systems or the received CDNR for IM/DD systems and the order of RBS, k, in the case of using identical optical modulation index (OMI) in every RBS. The number of the RBS connected in the system, N, is assumed to be 10. In the proposed ROC systems, when all OMIs are set to be equal to each other, the CNR of the signal from the RBS nearest to a CS is smaller than those from other RBSs. This is because the optical carrier left to this RBS has the smallest power due to its use for modulation in previous RBSs. In the case of setting an equal value to all OMIs, therefore, we set the OMI to be the one which maximizes the CNR of the RBS nearest to the CS. If the OMI is too small, although the optical carrier left to the nearest RBS is still large, but the CNR of this RBS is small due to the small value of OMI. If the OMI is too large, the optical carrier left to this RBS is small, thus the CNR of this RBS is small. The OMI of 0.036 in the ROC/HD system and 0.015 in the ROC/SHD system are obtained by the method above.

In the IM/DD system, the CDNR of the signal from the middle RBS in the link is the smallest because the cascaded connection generates the maximum value of intermodulation distortion in the middle subcarrier frequency band (see Appendix). In this calculation, the OMI of 0.041 is the one which maximizes CDNR of the middle RBS. If the OMI is higher than this value, the CDNR is degraded by the intermodulation distortion.

It can be seen that the received CNR of the ROC/SHD system is about 1 dB less than that of the ROC/HD system. This is due to the fact that, in the ROC/SHD system, the received power of the pilot carrier which is utilized as the local oscillator, is decreased but not much because the OMI of each RBS is very small.

Table 1 Parameters used in calculations.

Parameter	Value
Local Light Power: P_L	10 dBm
Relative Intensity Noise: RIN	-152 dB/Hz
Photodiode responsivity: r (= eα)	0.8 A/W
Load Resistance: R_L	50 Ω
Noise Temperature: T	300 K

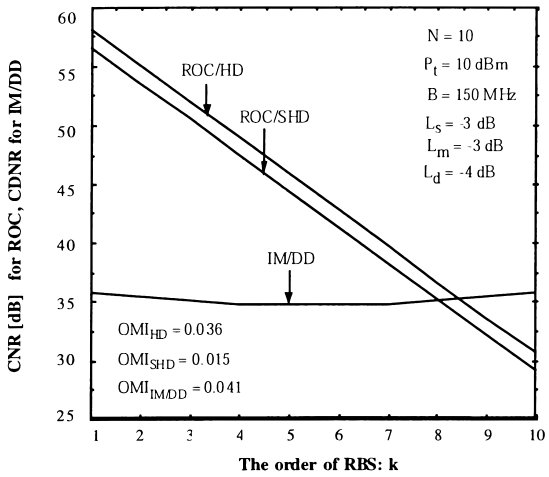

Fig. 4 Relationship between the received CDNR and the order of RBS in the case of using identical OMI in every RBS.

4.2 Optimization of Optical Modulation Indices

If we set the OMI of each RBS so that the OMI of the RBS farther from the CS is smaller than those of the RBSs nearer to the CS, the received CNR of the signal from the RBS far from the CS will decrease, and that of the signal from the RBS near to the CS will increase. Therefore we can optimize the received CNR performance in the sense that we set each OMI differently so that the received CNR of the RBS nearest to the CS increase and equals that of the RBS farthest from the CS. Hence, to determine each OMI, we get

$$CNR_k = CNR_{k+1} \quad (k = 1, 2, \ldots, N-1) \quad (24)$$

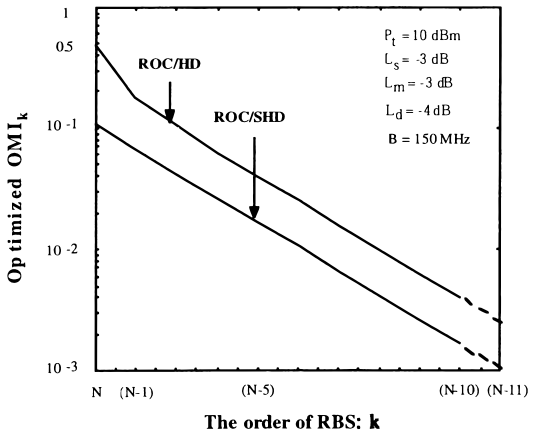

Fig. 5 Relationship between the optimized OMI and the order of RBS.

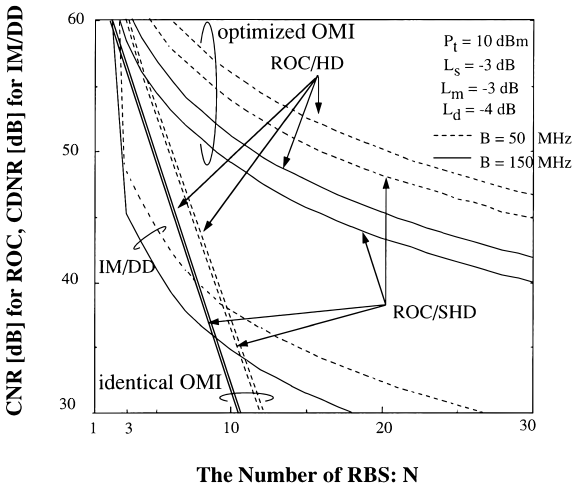

Fig. 6 Relationship between the received CDNR and the number of connected RBS.

From the relation above, in the case of both ROC/HD and ROC/SHD systems, it can be expressed as follows:

$$(\sin \pi OMI_k)^2 = L_m(\sin \pi OMI_{k+1})^2(\cos \pi OMI_k)^2 \quad (25)$$

Thus, the optimum OMI of the k-th RBS can be expressed as

$$OMI_k = \frac{1}{\pi} \arctan\left(\sqrt{L_m} \cdot \sin \pi OMI_{k+1}\right) \quad (26)$$

To determine the optimum OMIs, we start from setting the OMI of the N-th RBS which is nearest to the CS, and then use Eq. (26) to determine the OMIs of the $(N-1)$-th, $(N-2)$-th, ..., and 1st RBS, respectively. In the ROC/HD system, the OMI of the N-th RBS is firstly set to 0.5, i.e. using up the whole optical pilot carrier to achieve the maximum received CNR. In the ROC/SHD system, however, the received CNR also depends on the received power of the optical pilot carrier as shown in Eq. (21). Therefore the OMI of the N-th RBS should be set to a certain value to remain the appropriate power in the optical pilot carrier for self-heterodyne detection. In this calculation, the OMI of the N-th RBS in the ROC/SHD system which maximizes the received CNR is found to be 0.11 because the signal-ASE beat noise is dominant.

Figure 5 shows the relationship between the optimized OMI and the order of RBS in the case of ROC modulator insertion loss of 3 dB. It can be seen that the farther the RBS is located from the CS, the smaller the OMI of that RBS becomes, so that there is still enough power of the optical carrier left to the RBS nearer to the CS. It can also be seen that if a new RBS is added to the RBS farthest from the CS, we just have to set the optimum OMI of the new RBS without any change in other OMIs.

Figure 6 shows the relationship between the received CNR for ROC systems or the received CDNR for IM/DD systems and the number of RBSs with the radio signal bandwidth as a parameter. Here, the OMIs of the ROC systems are optimized using the proposed OMI optimization method. As a result, the received CNR of the RBS nearest to the CS in the case of using optimized OMIs shows a significant improvement over that in the case of using identical OMIs. The ROC systems using optimized OMIs also provide improvement in the received CNR over the CDNR of the IM/DD system, this is because the intermodulation distortion due to cascaded connection occurs in the IM/DD system when the number of RBSs is more than two, deteriorating the received CDNR severely. In the case of radio signal bandwidth, B, of 150 MHz and $N = 20$, the ROC/HD and the ROC/SHD systems provide approximately 16 dB and 14 dB improvement over the IM/DD system, respectively. The difference between the received CNR of the ROC/HD system and the ROC/SHD system is approximately 2 dB which is the larger than that in the case of using identical OMI for every RBS. This is due to the fact that the entire pilot carrier cannot be used up to achieve the maximum received CNR performance for the ROC/HD system in the case of using identical OMI. In the case of $B = 50$ MHz and $N = 20$, the ROC/HD and the ROC/SHD systems provide approximately 18 dB and 16 dB improvement over the IM/DD system, respectively. The improvement is better than that in the case of $B = 150$ MHz. This is because as B decreases, the received CDNR of the IM/DD system become higher not as much as that in the ROC systems, due to the intermodulation distortion.

In the case of adding a new RBS to the RBS farthest from a CS, the optimized OMI for the new RBS has already been derived by the proposed method, and no OMI re-optimization of the rest of the RBSs is required. On the other hand, in the case of adding a new RBS between any two RBSs, how to determine the OMI for the new RBS is to use the average value of the OMIs of its neighbor RBSs. This may be a sub-

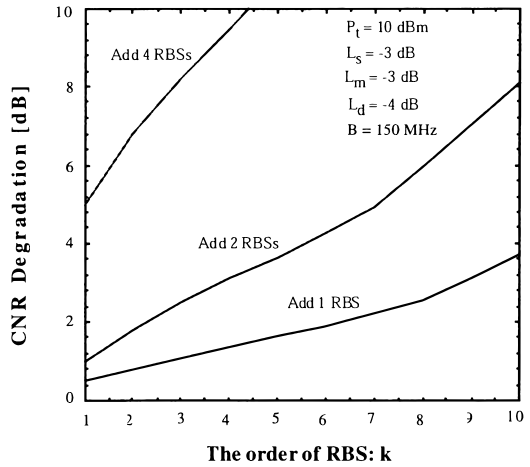

Fig. 7 Relationship between the received CNR degradation and the order of RBS in the case of adding new RBSs in ROC/HD system, and using the sub-optimum OMIs instead of re-optimization (One, two, or four RBSs are added in a 10-RBS system behind the RBS number shown in the horizontal axis).

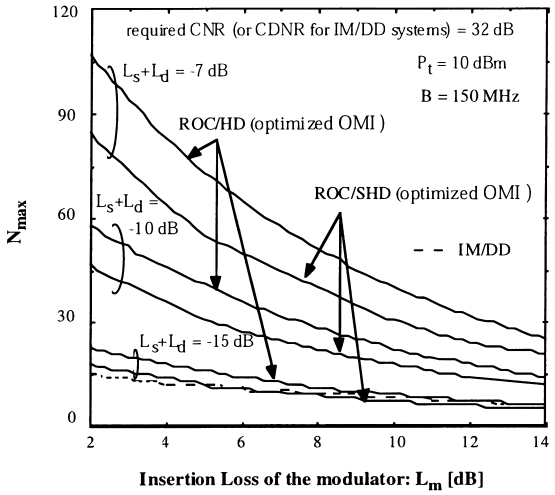

Fig. 8 Relationship between the maximum connected number of RBSs and the insertion loss of the modulator.

optimum value. Figure 7 shows the relationship between the received CNR degradation and the order of RBS in the case of adding new RBSs in the ROC/HD system, and using the sub-optimum OMIs instead of re-optimization. One, two, or four RBSs are added in a 10-RBS system behind the RBS number shown in the horizontal axis. Here, the CNR degradation means the degradation from the CNR obtained in the case of re-optimizing the OMIs. It is seen from this figure that the CNR degradation occurs when sub-optimum values of OMIs are used. In the ROC/SHD system, the CNR degradation occurs in a very similar pattern as that in the ROC/HD system. We can compensate this degradation by two methods. One method is to prepare a margin in the transmitting optical power level. That is, the transmitting optical power is set below its maximum power in the beginning, and then is increased when new RBSs is added. The other one is re-optimization of the OMIs. The former method may be used first, and when the transmitting optical power reaches its maximum available level, the re-optimization is performed.

In addition, the selection of the compensation method depends on the location of the added RBS. As shown in Fig. 7, without re-optimization, fewer RBSs can be added to the RBSs located near the CS because the OMIs of these RBSs are relatively high, thus assigning an average value of OMI of two neighbor RBSs to the new OMI without re-optimization deteriorates the CNR more severely in this region. Re-optimization should be more appropriate in this case.

Figure 8 shows the relationship between the maximum connected number of RBSs and the insertion loss of the optical modulator. Since the IM/DD system has only the loss of the modulator, therefore, to compare the proposed system with the IM/DD system fairly, only the loss of the modulator is expressed on the horizontal axis. In this calculation, it is assumed that the required CNR (CDNR for IM/DD systems) is 32 dB including the margin of 20 dB. This required CNR corresponds with the value to obtain the required bit error probability of 10^{-6} for a quarternary phase shift keying (QPSK) signal. We can see that, the ROC/HD and ROC/SHD systems using optimized OMIs can accommodate much more RBSs than the IM/DD system even in the relatively high insertion loss of the modulator region. The ROC/SHD system, for example, can accommodate at least 2 times as many RBSs as the IM/DD system in the case of total loss of the PC, FS and FC of 10 dB. The performance of ROC systems reduces to approximately same level as IM/DD systems when total loss of the PC, FS and FC is 15 dB.

Regarding the nonlinearity of each modulator, although the effects are not exactly the same in the proposed systems and the IM/DD system, it is a common factor in both systems. Hence, in order to analyze the fundamental merit of the proposed system, it is ignored in this study. Therefore, this paper does not include the nonlinearity in each modulator, RBS's receiver dynamic range, and the spurious characteristics.

5. Conclusion

We have newly proposed the novel radio-over-fiber systems using cascaded radio-to-optic direct conversion (ROC) scheme. We have theoretically analyzed the received CNR performance of the proposed systems using the cascaded ROC/HD scheme and the cascaded ROC/SHD scheme. The optimization of the optical modulation index in each RBS has also been presented. The following results are found:

(1) In the ROC/HD and ROC/SHD systems, the received CNR of the RBS nearest to the CS can be improved substantially by the proposed optical

modulation index optimization method.

(2) By using the proposed optical modulation index optimization method,

   (a) in the case of the RF signal bandwidth of 150 MHz and the number of RBS of 20, the ROC/HD and the ROC/SHD systems are shown to provide approximately 16 dB and 14 dB improvement of CNR over CDNR of the IM/DD system, respectively. This is because, in the IM/DD system, the intermodulation distortion due to cascaded connection of optical modulators occurs and deteriorates the received CDNR severely. On the other hand, no intermodulation distortion due to cascaded connection occurs in the proposed cascaded ROC systems.

   (b) ROC/HD and ROC/SHD systems using optimized OMIs can accommodate much more RBSs than the IM/DD system even in the relatively high insertion loss of the modulator region. The ROC/SHD system, for example, can accommodate at least 2 times as many RBSs as the IM/DD system in the case of total loss of the PC, FS and FC of 10 dB.

To realize the proposed systems, the optical nonlinear phenomena, four wavelength mixing, and so on, should be considered. In our future study, we will consider these phenomena and also evaluate the dynamic range concerning the intermodulation distortion in each ROC.

References

[1] S. Komaki, K. Tsukamoto, and M. Okada, "Multiband operation of multimedia mobile radio on the virtual radio free space network," Proc. 2nd International Workshop on MoMuS-2, vol.1, no.1, pp.1–4, April 1995.

[2] W.I. Way, "Optical fiber-based microcellular systems: An overview," IEICE Trans. Commun., vol.E76-B, no.9, pp.1091–1102, Sept. 1993.

[3] H. Harada, H.J. Lee, S. Komaki, and N. Morinaga, "Performance analysis of fiber-optic millimeter-wave band radio subscriber loop," IEICE Trans. Commun., vol.E76-B, no.9, pp.1128–1135, Sept. 1993.

[4] Y. Matsunaka and M. Shibutani, "A short-span optical feeder for wireless personal communication systems using multimode fibers," IEICE Trans. Electron., vol.E79-C, no.1, pp.118–123, Jan. 1996.

[5] G.H. Smith, D. Novak, and C. Lim, "A millimeter-wave full-duplex fiber-radio star-tree architecture incorporating WDM and SCM," IEEE Photon. Technol. Lett., vol.10, no.11, pp.1650–1652, Nov. 1998.

[6] S. Kajiya, K. Tsukamoto, and S. Komaki, "Proposal of fiber-optic radio highway networks using CDMA method," IEICE Trans. Electron., vol.E79-C, no.1, pp.111–117, Jan. 1996.

[7] Y. Shoji, K. Tsukamoto, M. Okada, and S. Komaki, "Fiber-optic radio access networks using photonic self-synchronized TDM bus link," Proc. The First International Symposium on Wireless Personal Multimedia Communications (WPMC'98), pp.145–150, Yokosuka, Japan, Nov. 1998.

[8] W. Domon, M. Shibutani, and K. Emura, "SCM optical multiple-access networks with cascaded optical modulators," IEEE Photon. Technol. Lett., vol.5, no.9, pp.1107–1109, Sept. 1993.

[9] T. Fujii, K. Tsukamoto, and N. Morinaga, "Optical multiaccess SCM/coherent detection system using cascade connected optical phase modulators," IEICE Technical Report, OCS93-26, June 1993.

[10] P. Suwonpanich, Y. Shoji, K. Tsukamoto, and S. Komaki, "Proposal of cascaded radio-optic direct conversion radio highway," Proc. 1997 Asia Pacific Microwave Conference (APMC'97), vol.1, pp.385–388, Hong Kong, Dec. 1997.

[11] P. Suwonpanich, Y. Shoji, K. Tsukamoto, and S. Komaki, "Study on cascaded radio-optic direct conversion radio highway using optical amplifier," Proc. 1998 Asia Pacific Microwave Conference (APMC'98), vol.1, pp.317–320, Yokohama, Japan, Dec. 1998.

[12] P. Suwonpanich, K. Tsukamoto, and S. Komaki, "Optimization of optical modulation indices in a cascaded radio-to-optic direct conversion radio highway," Proc. 1999 Microwave Photonics (MWP'99), pp.197–200, Melbourne, Australia, Nov. 1999.

[13] Y. Ishii, K. Tsukamoto, S. Komaki, and N. Morinaga, "Coherent fiber-optic microcellular radio communication system using a novel RF-to-optic conversion scheme," IEEE Trans. Microwave Theory & Tech., vol.43, no.9, pp.2241–2248, Sept. 1995.

[14] P. Suwonpanich, Y. Suda, K. Tsukamoto, and S. Komaki, "Theoretical CDNR analysis on radio-to-optic direct conversion SCM coherent radio-over-fibre system," Opt. Quantum Electron., vol.30, no.11–12, pp.1103–1117, Dec. 1998.

[15] J. Farre, E. Bodtker, G. Jacobsen, and K.E. Stubkjar, "Dynamic range of an optical amplifier cascade in an ASK system with significant phase noise," IEEE Photon. Technol. Lett., vol.4, no.12, pp.1354–1357, Dec. 1992.

[16] I.M.I. Habbab and J.L. Cimini, Jr., "Optimized performance of erbium-doped fiber amplifiers in subcarrier multiplexed lightwave," IEEE J. Lightwave Technol., vol.9, no.10, pp.1321–1329, Oct. 1991.

Appendix

Figure A·1 shows the configuration of the conventional cascaded IM/DD system. The loss between two adjacent amplifiers is given by

$$L_{sub-IM} = L_f L_m \qquad (\text{A}\cdot 1)$$

The gain of each optical amplifier is assumed to be identical to the loss between two adjacent optical amplifiers, thus

$$G_{IM} = \frac{1}{L_{sub-IM}} \quad \text{for all amplifiers} \qquad (\text{A}\cdot 2)$$

Therefore the power spectral density of the amplified spontaneous emission (ASE) received at the receiver is

$$N_{ASE-IM} = \frac{pn_{sp}(G-1)h\nu}{L_f} \qquad (\text{A}\cdot 3)$$

In the case of employing linearized intensity modulators, the received optical power at the photodiode is [8]

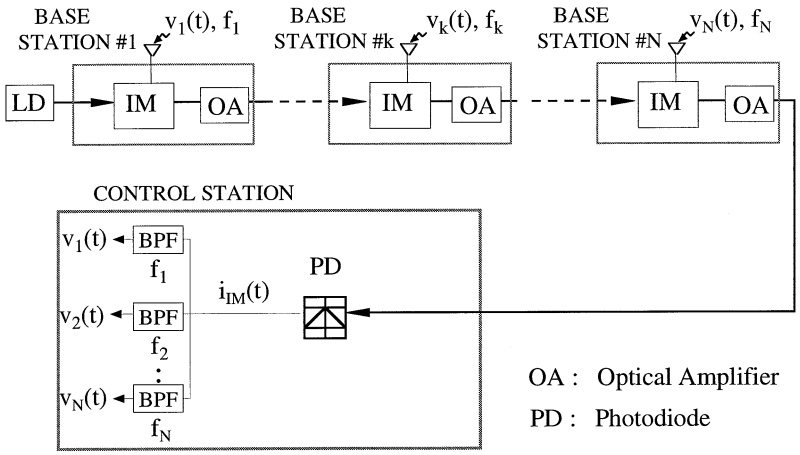

Fig. A· 1 Configuration of the conventional cascaded IM/DD system.

$$P_N = L_f P_t \prod_{i=1}^{N}(1 + OMI \sin \omega_i t)$$
$$= L_f P_t \left\{ 1 + OMI \sum_i \sin \omega_i t + \left(\frac{OMI^2}{2}\right) \cdot \sum_{i_1 \neq} \sum_{i_2} \cos(\omega_{i1} \pm \omega_{i2})t + \left(\frac{OMI^3}{4}\right) \cdot \sum_{i_1 \neq} \sum_{i_2 \neq} \sum_{i_3} \sin(\omega_{i1} \pm \omega_{i2} \pm \omega_{i3})t + \ldots \right\} \quad (A\cdot 4)$$

the received CDNR of each RF signal is

$$CDNR_{IM} = \frac{\frac{1}{2}e^2\alpha^2(P_t L_f)^2 OMI^2}{\sigma^2_{noise} + \sigma^2_{IM3}} \quad (A\cdot 5)$$

where σ^2_{noise} is the total noise power and σ^2_{IM3} is the power of the third-order intermodulation distortion (IM3) expressed by, respectively

$$\sigma^2_{noise} = \{RINe^2\alpha^2(P_t L_f)^2 + 2e^2\alpha(P_t L_f) + 2e^2\alpha N_{ASE} B_o + \frac{4k_B T}{R_L} + 4e^2\alpha^2(P_t L_f)N_{ASE} + 4e^2\alpha^2 N^2_{ASE} B_o\}B \quad (A\cdot 6)$$

$$\sigma^2_{IM3} = \frac{1}{2}e^2\alpha^2(P_t L_f)^2 \left(\frac{OMI^3 D_3(N,k)}{4}\right)^2 \quad (A\cdot 7)$$

where k is the order of RBS and $D_3(N,k)$ is the number of three-tone IM3 given by

$$D_3(N,k) = \frac{k}{2}(N-k+1) + \frac{1}{4}\{(N-3)^2 - 5\} - \frac{1}{8}\{1-(-1)^N\}(-1)^{N+k} \quad (A\cdot 8)$$

The CDNR of the signal from each RBS is not equal because the number of the third order intermodulation distortion is different in each subcarrier channel. Since the number of the third order intermodulation distortion reaches maximum in the middle channel, the CDNR of the middle RBS is the smallest.

Pat Suwonpanich was born in New York, USA, on August 22, 1974. He received the B.E. degree in Electrical Engineering from Chulalongkorn University, Bangkok, Thailand in 1994, and M.E. degree in Communication Engineering from Osaka University in 1998. He is currently pursuing Ph.D. degree at Osaka University. He is engaging in research on radio and optical communication systems.

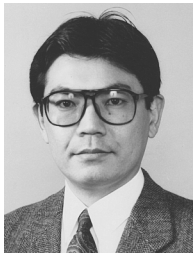

Katsutoshi Tsukamoto was born in Shiga, Japan in October 7, 1959. He received B.E., M.E. and Ph.D. degrees in Communication Engineering from Osaka University, in 1982, 1984 and 1995 respectively. He is currently an Associate Professor in the Department of Communications Engineering at Osaka University, engaging in the research on radio and optical communication systems. He is a member of IEEE.

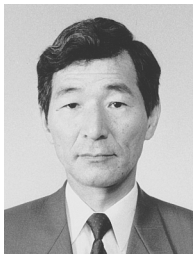

Shozo Komaki was born in Osaka, Japan in 1947. He received B.E., M.E. and D.E. degrees in Electrical Communication Engineering from Osaka University, in 1970, 1972 and 1983 respectively. In 1972, he joined the NTT Radio Communication Labs., where he was engaged in repeater development for a 20 GHz digital radio system, 16-QAM and 256-QAM systems. From 1990, he moved to Osaka University, Faculty of Engineering, and engaging in the research on radio and optical communication systems. He is currently a Professor of Osaka University. Dr. Komaki is a senior member of IEEE and the Institute of Television Engineers of Japan (ITE). He was awarded the Paper Award and the Achievement Award of IEICE, Japan in 1977 and 1994 respectively.